IEEE Access
Multidisciplinary | Rapid Review | Open Access Journal

Received April 28, 2020, accepted May 11, 2020, date of publication May 19, 2020, date of current version June 2, 2020.

Digital Object Identifier 10.1109/ACCESS.2020.2995672

An Adaptive Turn Rate Estimation for Tracking a Maneuvering Target

MOHAMED ELTOUKHY, M. OMAIR AHMAD, (Life Fellow, IEEE), AND M. N. S. SWAMY, (Life Fellow, IEEE)
Department of Electrical and Computer Engineering, Concordia University, Montreal, QC H3G1M8, Canada

Corresponding author: Mohamed Eltoukhy (m_eltou@ece.concordia.ca)

This work was supported in part by the Natural Sciences and Engineering Research Council (NSERC) of Canada, and in part by the Regroupement Stratgique en Microlectronique du Qubec (ReSMiQ).

ABSTRACT Tracking maneuvering targets accurately is one of the most challenging tasks in the design of aircraft tracking systems. For efficient tracking performance, the target motion predicted by the target motion model needs to match the target's actual motion during the maneuver. For tracking a maneuvering target, a combination of the constant velocity (CV) model and the coordinated turn (CT) model with a known turn rate are incorporated in the interacting multiple model (IMM) algorithm. However, in such a scheme when a target performs an unexpected maneuver, the tracking performance deteriorates, or the scheme may even fail to track the target. To overcome this problem, there exists a scheme in the literature, in which instead of using an *a priori* knowledge of the target turn rate, it is estimated adaptively using the target acceleration and speed. However, this algorithm uses a three-dimensional model to estimate the turn rate in two-dimensional space, which may result in an inaccurate estimation of the target acceleration, and thus may lead to in inaccurate turn rate value. In this paper, an adaptive algorithm to track a maneuvering target in an IMM framework is proposed. Estimating the turn rate is based on the speed of the target and the radius of the turn, where the latter is computed by a simple method using the previous three successive measurements. Further, a detailed study to select an appropriate transition probability matrix for the proposed algorithm is carried out. Simulation results demonstrate that the proposed tracking algorithm outperforms the other algorithms in terms of its tracking accuracy and consistency, particularly in the realistic situation when neither an *a priori* knowledge about the target turn rate nor about the range rate information is available to the tracking algorithm.

INDEX TERMS Interacting multiple model for radar tracking, target tracking, target turn rate estimation, maneuvering targets.

I. INTRODUCTION

One of the major challenges faced by any target tracking system is to track targets during maneuverability, i.e., when the aircraft turns right or left with a certain angle. Two approaches have been used for tracking a maneuvering target. One of them uses a maneuver detector and the other does not. The maneuver detector is a statistical test, which is formulated to decide whether the target maneuver has begun or not. Same framework is used to test whether the maneuver has ended or not [1].

In the first approach, the algorithm uses a single filter in all the tracking process. The algorithm is assumed to track the target in the non-maneuvering mode, when the detector decides that a maneuver is begun, the algorithm switches to track the target in the maneuvering mode. One of the most basic algorithms in this approach uses the two-level white noise filter [2], in which the filter models the target motion with a constant velocity (CV) and switches between two noise levels, the low noise level for the non-maneuvering mode and the high noise level for the maneuvering mode. Another algorithm in the maneuver-detector approach is the variable dimension (VD) algorithm [3]. This algorithm also uses one filter and utilizes two motion models: the CV model is used for the non-maneuvering motion of the target, and the constant acceleration (CA) model for the maneuvering motion. In general, the algorithms in this approach show a high peak position error at the beginning of the maneuver

The associate editor coordinating the review of this manuscript and approving it for publication was Zhixiong Peter Li.

motion, which may be higher than the raw measurement data [3].

The second approach is to track the target without a maneuver detector. In this approach, a number of filters are used in parallel, each of which uses a different motion model. The output is a weighted sum of the outputs of these filters. These weights are proportional to the probability of each filter being the accurate one to track this target [4]. This approach overcomes the problem of peak position error that appears in the maneuver-detector algorithms [5], [6]. Several algorithms have been proposed in this approach such as the first order generalized pseudo-Bayesian (GPB1), the second order of GPB (GPB2), and interacting multiple model (IMM) [7]–[11]. The IMM algorithm has a slightly higher complexity, but a better performance compared to that of GPB1 algorithm and significantly lower complexity than GPB2 with a comparable tracking performance [12]. The implementation of IMM with a large number of filters does not guarantee a better performance, despite its increased complexity [13]. This algorithm shows an efficient tracking performance when it utilizes the CV model and coordinated turn (CT) model with known turn rate [14], [15]. However, the tracking performance deteriorates when the turn rates deviate from the maneuver performed by the target, i.e., a prior information about the target maneuver is required for better tracking performance [16].

For a practical implementation of the IMM algorithm, we have to determine the turn rate, since it is not known. The first method assumes that the maneuver range that will be performed by the target is known *a priori* [17], and the turn rate is selected to cover these expected maneuvers, but the tracking performance degrades if this prior knowledge of the range is inaccurate. The second method obtains the turn rate by estimating the magnitude of target acceleration and speed [18]. In general, the estimated accelerations may not be precise and may cause biased estimation of the turn rate. In the third method, the turn rate is included in the state vector and is estimated along with the other elements of the state vector [5], [19]. This results in a nonlinear CT model, which is computationally more expensive to estimate the elements of the state vector. Recently, it has been proposed that the range rate information can be used to improve the turn rate estimation [20]–[22]. However, this information may not be available in all radar types [16].

In this work, it is assumed that the target performs the maneuver in a uniform circular motion in two-dimensional plane with a constant speed, as mentioned in [23]. The framework of IMM with three filters is used. One of these filters uses the CV model and the other two use the CT model, one of which is to track the target for the right turn and the other for the left turn [24]. In this algorithm, the turn rate of the target is adaptively estimated at each time step without any prior knowledge about the target maneuverability or the range rate. The turn rate is based on the estimation of the radius of the turn and the speed of the target and is calculated as the speed of the target divided by the radius of the turn. The performance of the proposed algorithm is evaluated and compared with two other types of IMM tracking algorithms that use linear models. One of these types uses a known turn rate, whereas the other adaptively estimates it using the speed and acceleration. These algorithms are evaluated in various maneuvers in terms of the normalized position error [18] and estimator consistency [25].

This manuscript is organized as follows: Section II introduce the state space model (the target motion and measurement models used in this work). A brief review of the IMM algorithm is provided in Section III. In Section IV, we introduce the proposed algorithm wherein a method of estimating the turn rate is given. Section V is devoted to the performance evaluation and comparison of the results with that of the other existing linear IMM algorithms. Finally, Section VI contains the conclusions.

II. THE STATE SPACE MODEL

The precision of the target motion model is crucial to the tracking accuracy of a tracker, in that the performance of the tracker deteriorates if there is a mismatch between the motion predicted by the assumed model and the actual motion of the target. Assuming the target performs a two-dimensional motion and a CT maneuver, the target kinematics may be represented by its position and velocity, and the target state vector is given by

$$\mathbf{x}_k = [\xi_k,\ \dot{\xi}_k,\ \eta_k,\ \dot{\eta}_k]' \tag{1}$$

where ξ_k and η_k represent the target's position in the x and y directions, respectively, $\dot{\xi}_k$ and $\dot{\eta}_k$ are the corresponding target velocity components, and $(\cdot)'$ denotes the transpose. The equation of the state-space model that describes the target motion is given by [26].

$$\mathbf{x}_k = \mathbf{F}_{k-1}\mathbf{x}_{k-1} + \Gamma\mathbf{w}_{k-1} \tag{2}$$

where $\mathbf{F}_{k-1}$ is the state transition matrix and Γ is the disturbance matrix that can be expressed as

$$\Gamma = \begin{bmatrix} 0.5T^2 & 0 \\ T & 0 \\ 0 & 0.5T^2 \\ 0 & T \end{bmatrix} \tag{3}$$

where T is the sampling period. Generally, radar systems provide the measurements in polar coordinates, that is, in terms of azimuth and range. However, tracking using polar coordinates is not as accurate as tracking using Cartesian coordinates and hence the latter is recommended with a suitable measurement conversion [27]. Therefore, using a suitable conversion of the polar measurement such as used in [28], we can track the target in Cartesian coordinates for better tracking performance. Therefore, most of the algorithms that have been proposed for target tracking assume that suitable conversion has already been made of the polar measurement to Cartesian coordinates [5], [11], [15], [18]. We have also followed the same practice as others have done. Then,

the measurement equation is given by

$$\mathbf{z}_k = \mathbf{H}_k \mathbf{x}_k + \mathbf{m}_k \tag{4}$$

with the measurement matrix

$$\mathbf{H}_k = \begin{bmatrix} 1 & 0 & 0 & 0 \\ 0 & 0 & 1 & 0 \end{bmatrix} \tag{5}$$

where $\mathbf{z}_k$ is the received measurement, $\Gamma\mathbf{w}_{k-1}$, and $\mathbf{m}_k$ are the additive white Gaussian process and measurement noise vectors, respectively. Conventionally, $\Gamma\mathbf{w}_{k-1}$ and $\mathbf{m}_k$ are assumed to be independent with zero mean and with covariance matrices $\Gamma\mathbf{Q}_{k-1}\Gamma'$ and $\mathbf{C}_k$, respectively.

When the target performs a straight-line motion at a constant velocity, the state transition matrix ($\mathbf{F}_k = \mathbf{F}_k^{CV}$) is given by [26]

$$\mathbf{F}_k^{CV} = \begin{bmatrix} 1 & T & 0 & 0 \\ 0 & 1 & 0 & 0 \\ 0 & 0 & 1 & T \\ 0 & 0 & 0 & 1 \end{bmatrix} \tag{6}$$

where $\mathbf{F}_k^{CV}$ corresponds to the CV model. When it performs a CT motion with a known turn rate ω, the state transition matrix ($\mathbf{F}_k = \mathbf{F}_k^{CT}$) is given by [29]

$$\mathbf{F}_k^{CT} = \begin{bmatrix} 1 & \dfrac{\sin(\omega T)}{\omega} & 0 & -\dfrac{1-\cos(\omega T)}{\omega} \\ 0 & \cos(\omega T) & 0 & -\sin(\omega T) \\ 0 & \dfrac{1-\cos(\omega T)}{\omega} & 1 & \dfrac{\sin(\omega T)}{\omega} \\ 0 & \sin(\omega T) & 0 & \cos(\omega T) \end{bmatrix} \tag{7}$$

This corresponds to the CT model with a known turn rate.

III. THE IMM ALGORITHM

The IMM algorithm is quite effective in tracking a maneuvering target, wherein the target maneuver is modeled as a combination of different motion models. The output at each time step is a combination of the outputs of all the filters weighted by the corresponding mode probability, the mode probability being defined as the probability of the model matching the target motion. At each time step, the algorithm decides as to which model is suitable to predict the motion of the target (non-maneuvering or maneuvering motion) based on the mode probability. The block diagram of a single cycle of the IMM algorithm, which uses two Kalman filters each using a different motion model, is shown in Fig. 1 [14].

The predicted state vector $\tilde{\mathbf{x}}_k^j$ for a Kalman filter j is given by [30]

$$\tilde{\mathbf{x}}_k^j = \mathbf{F}_{k-1}\hat{\mathbf{x}}_{k-1}^{oj} \tag{8}$$

where $\hat{\mathbf{x}}_{k-1}^{oj}$ is the input state vector for the filter j. The predicted error covariance matrix, $\tilde{\mathbf{P}}_k^j$, is given by

$$\tilde{\mathbf{P}}_k^j = \mathbf{F}_{k-1}\hat{\mathbf{P}}_{k-1}^{oj}\mathbf{F}_{k-1}' + \Gamma\mathbf{Q}_{k-1}\Gamma' \tag{9}$$

where $\hat{\mathbf{P}}_{k-1}^{oj}$ is the error covariance matrix of the input state vector for the filter j. The measurement innovation or the residual of the filter $\boldsymbol{\beta}_k^j$

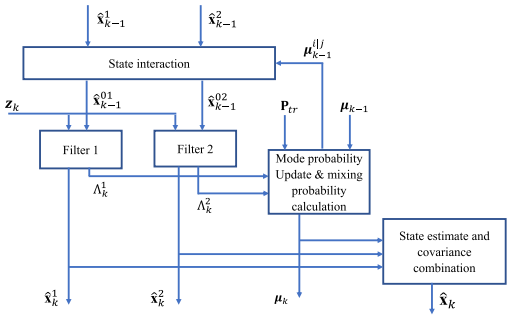

FIGURE 1. One cycle of the IMM algorithm when $r = 2$ [14].

$$\boldsymbol{\beta}_k^j = \mathbf{z}_k - \mathbf{H}_k\tilde{\mathbf{x}}_k^j \tag{10}$$

where $\mathbf{z}_k$ is the received measurement vector. The innovation error covariance matrix, $\mathbf{S}_k^j$, is given by

$$\mathbf{S}_k^j = \mathbf{H}_k\tilde{\mathbf{P}}_k^j\mathbf{H}_k' + \mathbf{C}_k \tag{11}$$

The Kalman gain $\mathbf{K}_k^j$ is defined as

$$\mathbf{K}_k^j = \tilde{\mathbf{P}}_k^j\mathbf{H}_k'(\mathbf{S}_k^j)^{-1} \tag{12}$$

The output state estimate $\hat{\mathbf{x}}_k^j$ of the Kalman filter j and its error covariance matrix $\hat{\mathbf{P}}_k^j$ are expressed as

$$\hat{\mathbf{x}}_k^j = \tilde{\mathbf{x}}_k^j + \mathbf{K}_k^j\boldsymbol{\beta}_k^j \tag{13}$$

$$\hat{\mathbf{P}}_k^j = [\mathbf{I} - \mathbf{K}_k^j\mathbf{H}_k]\tilde{\mathbf{P}}_k^j \tag{14}$$

where $\mathbf{I}$ is the identity matrix.

Assuming the IMM algorithm to contain only two Kalman filters, each of which is used to find the output state estimate of the target according to a specific type of motion (e.g. non-maneuvering, referred to as mode 1, and maneuvering mode, referred to as mode 2). The algorithm starts with initial values for the mode probabilities μ_{k-1}^1 and μ_{k-1}^2. In addition, a fixed matrix $\mathbf{P}_{tr}$ is assumed, whose (i,j)th element, p_{ij}, $i,j = 1, 2$, is the probability of transition from mode i to mode j, wherein the sum of the elements of each row in this matrix is unity. The mode probabilities as well as the transition probabilities are used to calculate the mixing probabilities $\mu_{k-1}^{i|j}(i,j = 1,2)$. These mixing probabilities along with the filter outputs $\hat{\mathbf{x}}_{k-1}^j, j = 1, 2$ of the previous cycle are utilized to calculate the inputs to the filters, $\hat{\mathbf{x}}_{k-1}^{0j}, j = 1, 2$. In other words, each filter input is calculated as a weighted sum of all the filter outputs of the previous cycle. When the new measurement $\mathbf{z}_k$ is received, each filter updates its output state, $\hat{\mathbf{x}}_k^1$ and $\hat{\mathbf{x}}_k^2$. Then, the likelihood probabilities of the filters, Λ_k^1 and Λ_k^2, are computed from the measurement innovation $\boldsymbol{\beta}_k$, and the corresponding covariance matrix $\mathbf{S}_k$ for each filter. Next, the mode probabilities are updated to μ_k^1 and μ_k^2, using Λ_k^1 and Λ_k^2, μ_{k-1}^1 and μ_{k-1}^2, and $\mathbf{P}_{tr}$. Finally, the output state estimate $\hat{\mathbf{x}}_k$ is computed as a weighted sum of the outputs of the filters using the weights of the updated mode probabilities,

μ_k^1 and μ_k^2. The outputs of the filters and the updated mode probabilities are set as the initial data for the next cycle. More details about the IMM algorithm can be found in [31]. The steps of the IMM algorithm with r filters are as follows

1) **State interaction**: In this step, the previous state estimates and their covariance matrices are mixed using the calculated mixing probabilities $\mu_{k-1}^{i|j}$. The input state vector of the jth filter, $\hat{\mathbf{x}}_{k-1}^{oj}$ and its covariance matrix $\hat{\mathbf{P}}_{k-1}^{oj}$ are calculated as

$$\hat{\mathbf{x}}_{k-1}^{oj} = \sum_{i=1}^{r} \hat{\mathbf{x}}_{k-1}^{i} \mu_{k-1}^{i|j} \quad i,j = 1, \cdots, r \tag{15}$$

and

$$\hat{\mathbf{P}}_{k-1}^{oj} = \sum_{i=1}^{r} \mu_{k-1}^{i|j} [\hat{\mathbf{P}}_{k-1}^{i} + [\hat{\mathbf{x}}_{k-1}^{i} - \hat{\mathbf{x}}_{k-1}^{oj}] \times [\hat{\mathbf{x}}_{k-1}^{i} - \hat{\mathbf{x}}_{k-1}^{oj}]'], \quad i,j = 1, \cdots, r \tag{16}$$

where

$$\mu_{k-1}^{i|j} = \frac{1}{\bar{e}^j} p^{ij} \mu_{k-1}^{i}, \quad i,j = 1, \cdots, r \tag{17}$$

with the normalization constant

$$\bar{e}^j = \sum_{i=1}^{r} p_{ij} \mu_{k-1}^{i}, \quad i,j = 1, \cdots, r \tag{18}$$

2) **Mode probability update**: when the measurement $\mathbf{z}_k$ is received, each Kalman filter uses its input state and its error covariance matrix to calculate its output state $\hat{\mathbf{x}}_k^j$ and its error covariance matrix $\hat{\mathbf{P}}_k^j$. Moreover, both the innovation $\boldsymbol{\beta}_k^j$ and its error covariance matrix $\mathbf{S}_k^j$ [30] are used to calculate the likelihood of each filter, which is given by

$$\Lambda_k^j = \frac{1}{\sqrt{2\pi \mathbf{S}_k^j}} \exp[-0.5(\boldsymbol{\beta}_k^j)'(\mathbf{S}_k^j)(\boldsymbol{\beta}_k^j)], \quad j = 1, \cdots, r \tag{19}$$

Then, the mode probability update for the jth filter is computed as

$$\mu_k^j = \frac{1}{G} \Lambda_k^j \bar{e}^j, \quad j = 1, \cdots, r \tag{20}$$

and

$$G = \sum_{j=1}^{r} \Lambda_k^j \bar{e}^j \tag{21}$$

3) **Fusion of the outputs**: The output state estimate $\hat{\mathbf{x}}_k$ and its error covariance matrix $\hat{\mathbf{P}}_k$ are computed as a fusion of all the filter output states and their covariance matrices weighted by the updated model probabilities, respectively.

$$\hat{\mathbf{x}}_k = \sum_{j=1}^{r} \hat{\mathbf{x}}_k^j \mu_k^j \tag{22}$$

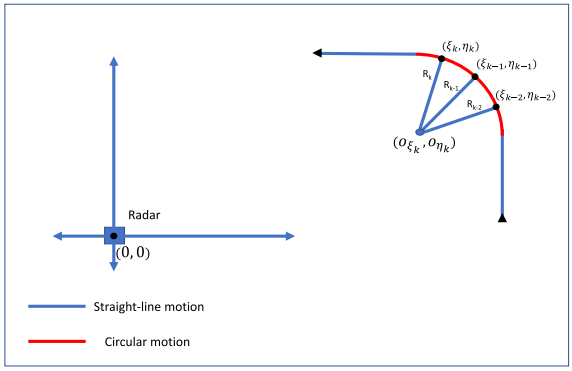

FIGURE 2. Target motions.

and

$$\hat{\mathbf{P}}_k = \sum_{j=1}^{r} \mu_k^j [\mathbf{P}_k^j + [\hat{\mathbf{x}}_k^j - \hat{\mathbf{x}}_k][\hat{\mathbf{x}}_k^j - \hat{\mathbf{x}}_k]'] \tag{23}$$

IV. THE PROPOSED TRACKING ALGORITHM

Consider a target that is moving in a circular path around a fixed center at a speed v in a 2-D space. Then its angular speed (or the turn rate) ω is given by [32], [33]

$$\omega = \frac{v}{R} \tag{24}$$

where R is the radius of the circle. If v is assumed to be constant, then angular speed, i.e., the turn rate is also constant. The speed v of the target can be calculated at each time step from the estimated velocity components in the output state estimate vector given by

$$v = \sqrt{\dot{\xi}^2 + \dot{\eta}^2} \tag{25}$$

where $\dot{\xi}$ and $\dot{\eta}$ are the velocity components in the x and y directions. Therefore, our aim is to estimate the radius R of the turn at a given instant.

For this purpose, we assume that the target motion consists of three sub-motions as depicted in Fig. 2. The sub-motions are two straight-line motions before and after the turn, and a circular motion during the turn with its center at (o_{ξ_k}, o_{η_k}). For the circular part of the motion, we assume that the target moves on the circumference of a circle with radius R_k, such that the received measurements are at the same distance from the center of the circle.

Suppose we have three consecutive measurements given by (ξ_{k-2}, η_{k-2}), (ξ_{k-1}, η_{k-1}), and (ξ_k, η_k). Then,

$$R_{k-2} = R_{k-1} = R_k \tag{26}$$

Then using the distance formula between two points and (26), we can determine (o_{ξ_k}, o_{η_k}), the coordinates of the center and then the radius R_k. The detailed proof is in Appendix A.

The block diagram of the proposed tracking IMM algorithm is shown in Fig. 3. The algorithm uses three Kalman filters, first of which uses the CV model to account for the straight-line motion of the target, and the second and third

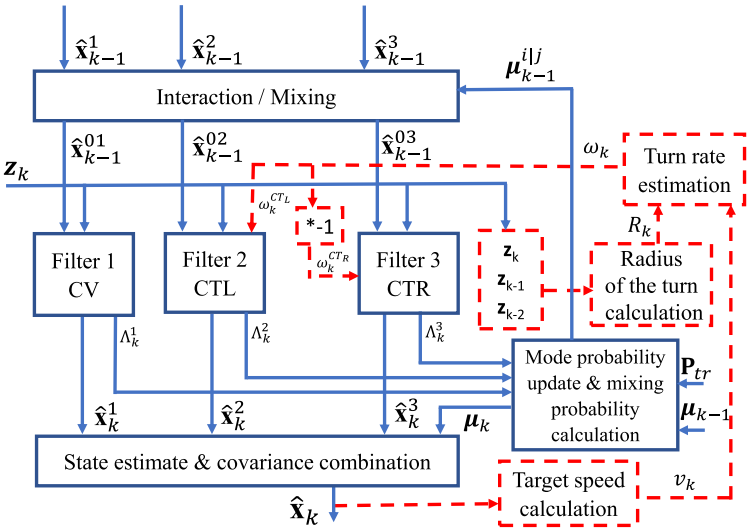

FIGURE 3. The block diagram of one cycle of the proposed tracking algorithm.

Algorithm 1 Determination of the Turn Rate ω_k

1: **Input**: (ξ_{k-2}, η_{k-2}), (ξ_{k-1}, η_{k-1}), (ξ_k, η_k), and $(\dot{\xi}_k, \dot{\eta}_k)$
2: **Find**: ω_k
3: **begin**
4: Obtain o_{ξ_k} using (A.5)
5: Obtain o_{η_k} using (A.7)
6: Obtain R_k using (A.8)
7: Obtain v_k using (25)
8: Obtain ω_k using (24)
9: **end**

filters, denoted by CTL and CTR filters, use the CT model to account for the left turning and right turning motions, respectively. For left turns, the estimated turn rate takes a positive sign, while negative values are used for the right turns [26]. A sign-changing block is located at the input of the CTR filter to switch the sign of the turn rate provided to the CT model in that filter to account for the right turn. The three measurements $\mathbf{z}_k$, $\mathbf{z}_{k-1}$, and $\mathbf{z}_{k-2}$ are fed to the block that calculates the radius R_k at the current time step, as shown in Fig. 3. Furthermore, the speed of the target is calculated from the output state estimate of the algorithm. This output state vector contains the estimated components for both the position and velocity of the target, where the target speed is calculated using (25). The output of the last two mentioned blocks, R_k and v_k, are then used to calculate the turn rate ω_k, which in turn is used in the next time step of the algorithm.

$$\omega_k^{CT_L} = \omega_k \tag{27}$$

$$\omega_k^{CT_R} = -\omega_k \tag{28}$$

where $\omega_k^{CT_L}$ and $\omega_k^{CT_R}$ are the left and right turn rates, respectively. Once $\omega_k^{CT_L}$ and $\omega_k^{CT_R}$ have been determined and the new measurement $\mathbf{z}_k$ is received, the measurement $\mathbf{z}_{k-2}$ is discarded, and the other two previous measurements $\mathbf{z}_{k-1}$ and $\mathbf{z}_k$ are retained as $\mathbf{z}_{k-2}$ and $\mathbf{z}_{k-1}$, respectively, and the process is repeated. The complete algorithm is given as Algorithm 2, wherein $\Gamma\mathbf{Q}\Gamma'$ and $\mathbf{C}$ are the covariance matrices for any

Algorithm 2 The Proposed Tracking Algorithm

1: **Input**: $\mathbf{P}_{tr}^{prop}$, Γ, $\mathbf{Q}$, $\mathbf{C}$, $\boldsymbol{\mu}_o$, $\omega_o^{CT_L}$, $\omega_o^{CT_R}$, N, and $\mathbf{z}_k$
2: **Find**: $\hat{\mathbf{x}}_k$ and $\hat{\mathbf{P}}_k$
3: **Initialization**: using $\mathbf{z}_1$ and $\mathbf{z}_2$, find $\hat{\mathbf{x}}_o$ and $\hat{\mathbf{P}}_o$ $\forall$ KF from (36) and (37)
4: **At k = 3, Set**:

$$\hat{\mathbf{x}}_{k-1}^1 = \hat{\mathbf{x}}_{k-1}^2 = \hat{\mathbf{x}}_{k-1}^3 = \hat{\mathbf{x}}_0$$
$$\hat{\mathbf{P}}_{k-1}^1 = \hat{\mathbf{P}}_{k-1}^2 = \hat{\mathbf{P}}_{k-1}^3 = \hat{\mathbf{P}}_o$$
$$\boldsymbol{\mu}_{k-1} = \boldsymbol{\mu}_o$$
$$\omega_{k-1}^{CT_L} = \omega_o^{CT_L}$$
$$\omega_{k-1}^{CT_R} = \omega_o^{CT_R}$$

5: **begin the process at k = 3 to N**
6: **for** j = 1:3 **do**
7: Obtain $\bar{e}^j$ and $\mu_{k-1}^{i|j}$ using (18) and (17)
8: Obtain $\hat{\mathbf{x}}_{k-1}^{oj}$ and $\hat{\mathbf{P}}_{k-1}^{oj}$ using (15) and (16)
9: Obtain $\hat{\mathbf{x}}_k^j$ and $\hat{\mathbf{P}}_k^j$ using (13) and (14) with $\omega_{k-1}^{CT_R}$ and $\omega_{k-1}^{CT_L}$
10: Obtain $\boldsymbol{\beta}_k^j$ and $\mathbf{S}_k^j$ using (10) and (11)
11: Obtain Λ_k^j using (19)
12: Obtain G and μ_k^j using (21) and (20)
13: **end for**
14: Compute $\hat{\mathbf{x}}_k$ and $\hat{\mathbf{P}}_k$ using (22) and (23)
15: Compute ω_k using Algorithm 1
16: Compute $\omega_k^{CT_L}$ and $\omega_k^{CT_R}$ using (27) and (28)
17: **end the process**

value of k, and

$$\mathbf{Q} = \begin{bmatrix} \sigma_Q^2 & 0 \\ 0 & \sigma_Q^2 \end{bmatrix} \tag{29}$$

$$\mathbf{C} = \begin{bmatrix} \sigma_C^2 & 0 \\ 0 & \sigma_C^2 \end{bmatrix} \tag{30}$$

where σ_Q and σ_C are, respectively, the standard deviations of the process noise and measurement noise in x or y directions.

It is to be pointed out that if only one KF is employed for the turning motion using the CT model, then the model can be designed either with a positive value or a negative value of the turn rate. For example, in the former case, the model can estimate the turn rate only for left turns, but will not be able to make a good estimate in the case of right turns. This is due to the fact that when the target performs a right turn, the algorithm will assign a higher weight to the KF with the CV model, thus resulting in a less accurate prediction of the target position. Hence, it is not appropriate to use only one KF for estimating both the right and left turn rates.

V. PERFORMANCE EVALUATION

In this section, the performance of the proposed algorithm as well as that of the existing linear IMM algorithms are compared and evaluated using the following metrics.

The normalized position error (NPE) [18] is used to compare the tracking accuracy of the position, and is given by

$$NPE_k = \frac{\sqrt{\frac{1}{M}\sum_{i=1}^{M}(\hat{\xi}_k^i - \xi_k^i)^2 + (\hat{\eta}_k^i - \eta_k^i)^2}}{\sqrt{\frac{1}{M}\sum_{i=1}^{M}(z_{\xi_k}^i - \xi_k^i)^2 + (z_{\eta_k}^i - \eta_k^i)^2}} \tag{31}$$

where $\hat{\xi}_k^i$ and $\hat{\eta}_k^i$ are the estimated positions in the x and y directions, respectively, while ξ_k^i and η_k^i are the corresponding true positions, $z_{\xi_k}^i$ and $z_{\eta_k}^i$ are the measured positions, and M is the number of runs performed in the Monte-Carlo simulation. When the value of NPE is less than unity, the estimator performance is acceptable; on the other hand, when it is not less than unity, the estimator performance is not acceptable, at this time step.

Another test to check whether the error of the state is well-suited with the corresponding covariance matrix of the estimated state or not, which is the average normalized estimation error squared (ANEES) test [28]. It is given by

$$ANEES_k = \frac{1}{Mn_x}\sum_{i=1}^{M}(\mathbf{x}_k^i - \hat{\mathbf{x}}_k^i)'(\hat{\mathbf{P}}_k^i)^{-1}(\mathbf{x}_k^i - \hat{\mathbf{x}}_k^i) \tag{32}$$

where $\mathbf{x}_k^i$ and $\hat{\mathbf{x}}_k^i$ are the true and estimated state vectors, respectively, and $\hat{\mathbf{P}}_k^i$ is the estimated error covariance matrix of the target at the time step k in the Monte-Carlo run number i, while n_x is the dimension of the state vector. The logarithmic ANEES (LANEES) is given by

$$LANEES_k = \log_{10}(ANEES_k) \tag{33}$$

is more expressive in terms of displaying the results [25]. When the value of LANEES is equal or less than zero, the estimator is said to be consistent at this time step.

For all the algorithms, the Kalman filters are initialized by using the first two consecutive measurements of the target position [16]. Let the first two consecutive measurements received be $\mathbf{z}_1$ and $\mathbf{z}_2$ given by

$$\mathbf{z}_1 = [z_{\xi_1}, z_{\eta_1}]' \tag{34}$$

$$\mathbf{z}_2 = [z_{\xi_2}, z_{\eta_2}]' \tag{35}$$

where z_{ξ_1} and z_{ξ_2} are the measured positions in the x direction at time $k = 1, 2$, respectively, while z_{η_1} and z_{η_2} are the measured positions in the y direction at time $k = 1, 2$, respectively. Then, the initial estimate state vector $\hat{\mathbf{x}}_o$ is given by

$$\hat{\mathbf{x}}_o = [z_{\xi_2}, \frac{z_{\xi_2} - z_{\xi_1}}{T}, z_{\eta_2}, \frac{z_{\eta_2} - z_{\eta_1}}{T}]' \tag{36}$$

where T is the sampling period. The initial error covariance matrix $\hat{\mathbf{P}}_o$ is given by [16]

$$\hat{\mathbf{P}}_o = \begin{bmatrix} \sigma_C^2 & \sigma_C^2/T & 0 & 0 \\ \sigma_C^2/T & 2\sigma_C^2/T^2 & 0 & 0 \\ 0 & 0 & \sigma_C^2 & \sigma_C^2/T \\ 0 & 0 & \sigma_C^2/T & 2\sigma_C^2/T^2 \end{bmatrix} \tag{37}$$

where σ_C is the standard deviation of the measurement noise. Assuming that the target moves nearly in a straight-line at the beginning of the tracking process, the initial mode probability is given by [18]

$$\boldsymbol{\mu}_o = \begin{cases} 0.6 & \textit{striaght line motion} \\ \dfrac{0.4}{r-1} & \textit{other motions} \end{cases} \tag{38}$$

where r is the total number of filters in each of the four IMM algorithms under consideration.

We use a sampling period T of 1 second, which conforms to the sampling period of modern radar systems [11]. The standard deviation σ_C of the measurement noise to be $10\,m$. Monte-Carlo simulations of 100 runs is performed assuming the noise for all the algorithms to be the same, for fair comparison.

The three algorithms that are used in the comparison are described below

The first algorithm, which we denote by A1, is an IMM algorithm that employs three filters; one of the filters uses the CV model and the other two the CT model with known turn rates of $\pm 2.5°/s$. The standard deviation for the process noise for all the models is assumed to be $0.003\,m/s^2$. The transition probability matrix of the algorithm is assumed as

$$\mathbf{P}_{tr}^{A1} = \begin{bmatrix} 0.9 & 0.05 & 0.05 \\ 0.05 & 0.9 & 0.05 \\ 0.05 & 0.05 & 0.9 \end{bmatrix} \tag{39}$$

The second algorithm, which we denote by A2, is the same as A1 except for the turn rates of the CT models that is assumed to be $\pm 3.5°/s$.

The third algorithm [18], which we denote as A3, is also an IMM algorithm but employs only two filters; one uses a CV model, and the other a turning rate model that utilizes

the target's position, velocity, and acceleration to estimate the target position, which we denote by 3CTR. The 3CTR model is given by [18]

$$\mathbf{F}^{3CTR} = \begin{bmatrix} \mathbf{A}_f & 0 \\ 0 & \mathbf{A}_f \end{bmatrix} \tag{40}$$

where

$$\mathbf{A}_f = \begin{bmatrix} 1 & \omega^{-1}\sin(\omega T) & \omega^{-2}(1-\cos(\omega T)) \\ 0 & \cos(\omega T) & \omega^{-1}\sin(\omega T) \\ 0 & -\omega\sin(\omega T) & \cos(\omega T) \end{bmatrix} \tag{41}$$

Its corresponding disturbance matrix can be expressed as

$$\Gamma_f = \begin{bmatrix} 0.167T^3 & 0 \\ 0.5T^2 & 0 \\ T & 0 \end{bmatrix} \tag{42}$$

The initial value of the turn rate is assumed to be $0.2°/s$. The standard deviation for the process noise for both the CV model and the 3CTR model is assumed to be $0.1\,m/s^2$ and $10.5\,m/s^2$, respectively, and the transition probability matrix of the algorithm to be [18]

$$\mathbf{P}_{tr}^{A3} = \begin{bmatrix} 0.98 & 0.02 \\ 0.02 & 0.98 \end{bmatrix} \tag{43}$$

In order to compare the performance of our algorithm with that of other two algorithms, we assume that the target moves at a speed of $100\,m/s$ with white Gaussian atmospheric noise having zero mean and standard deviation of $0.1\,m/s^2$ in both the x and y directions. The parameter (standard deviation) of the process noise is tuned to provide good tracking performance for given statistics of the atmospheric and measurement noises. In our proposed algorithm, it has been found that the standard deviation of the process noise of $0.003\,m/s^2$ for all the filters in all the scenarios for an atmospheric noise with a standard deviation of $0.1\,m/s^2$ and $10\,m$ for the standard deviation of measurement noise provides good performance. However, if the levels of the atmospheric and measurement noises change, the parameter of the process noise in the proposed algorithm needs to be re-tuned. After having considered a number of probability transition matrices, it has been found that the best transition probability matrix from the point of view of both NPE and LANEES is given by

$$\mathbf{P}_{tr}^{prop} = \begin{bmatrix} 0.9 & 0.05 & 0.05 \\ 0.1 & 0.8 & 0.1 \\ 0.1 & 0.1 & 0.8 \end{bmatrix} \tag{44}$$

For details regarding the above choice, see Appendix B. We choose the initial values of the turn rates of the two CT models to be $0.2°/s$ and $-0.2°/s$.

Comparison is now carried out under five scenarios, in which the targets performs various maneuvers. These scenarios along with the corresponding performance results in terms of NPE and consistency, as measured by LANEES, are shown in the sub-figures (a), (b), and (c), respectively, in Fig. 4 to Fig. 8.

In the first scenario, the target starts with a straight-line motion for 15 seconds, then performs the first maneuver to the left with a turn rate of $1.5°/s$ for 15 seconds. Afterwards, it moves again in a straight-line motion for 10 seconds, and then performs another turn to the left with a turn rate of $2.5°/s$ for 30 seconds. Finally, it goes in a straight-line motion for a

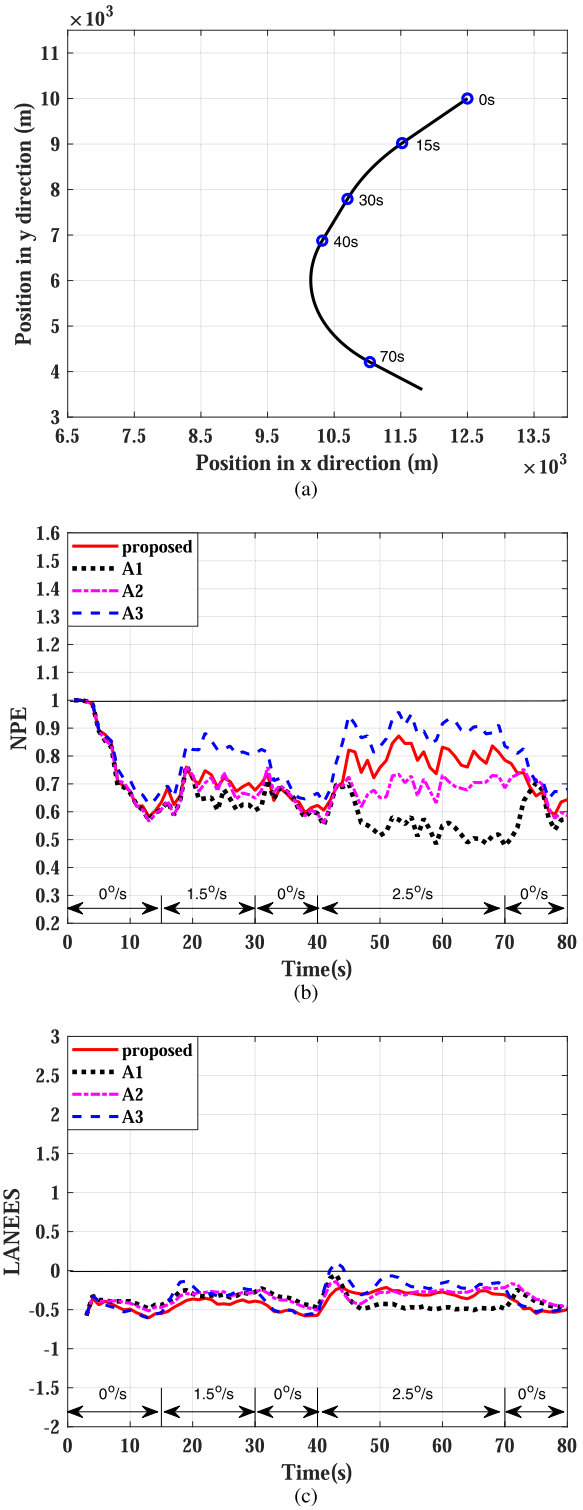

FIGURE 4. The results of the first scenario for a target that performs turns of $1.5°/s$, and $2.5°/s$. (a) True target trajectory. (b) Normalized position error. (c) Consistency test.

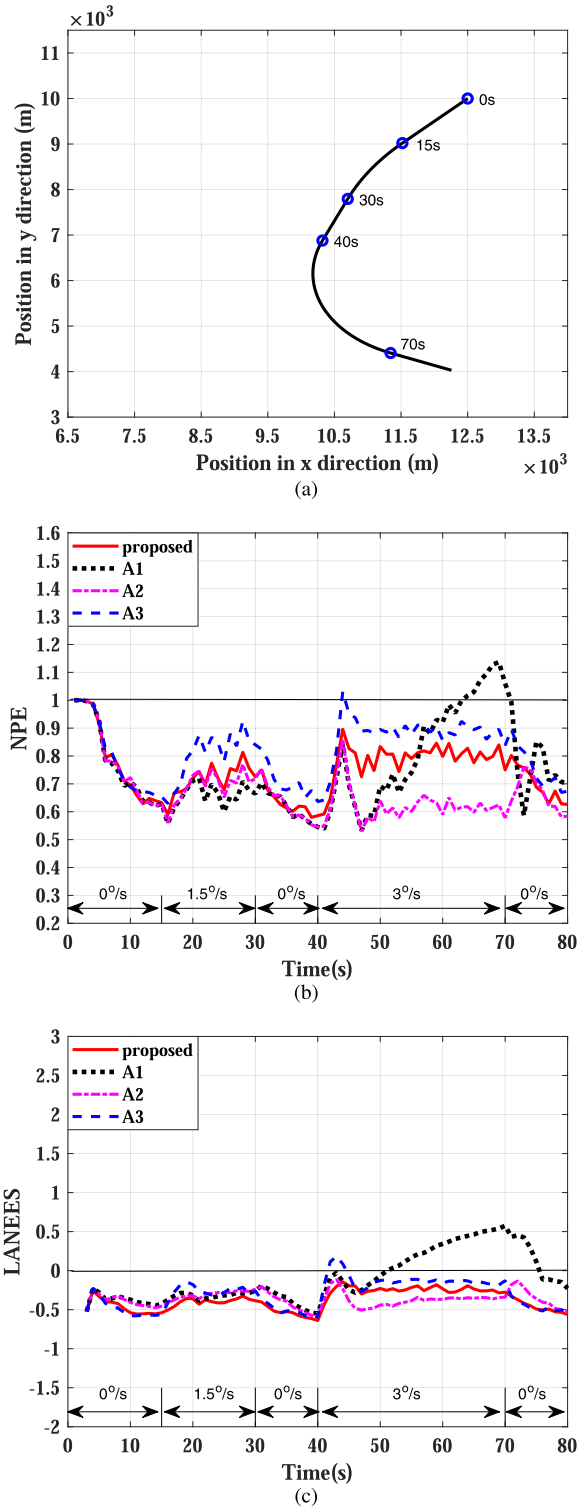

FIGURE 5. The results of the second scenario for a target that performs turns of 1.5°/s, and 3°/s. (a) True target trajectory. (b) Normalized position error. (c) Consistency test.

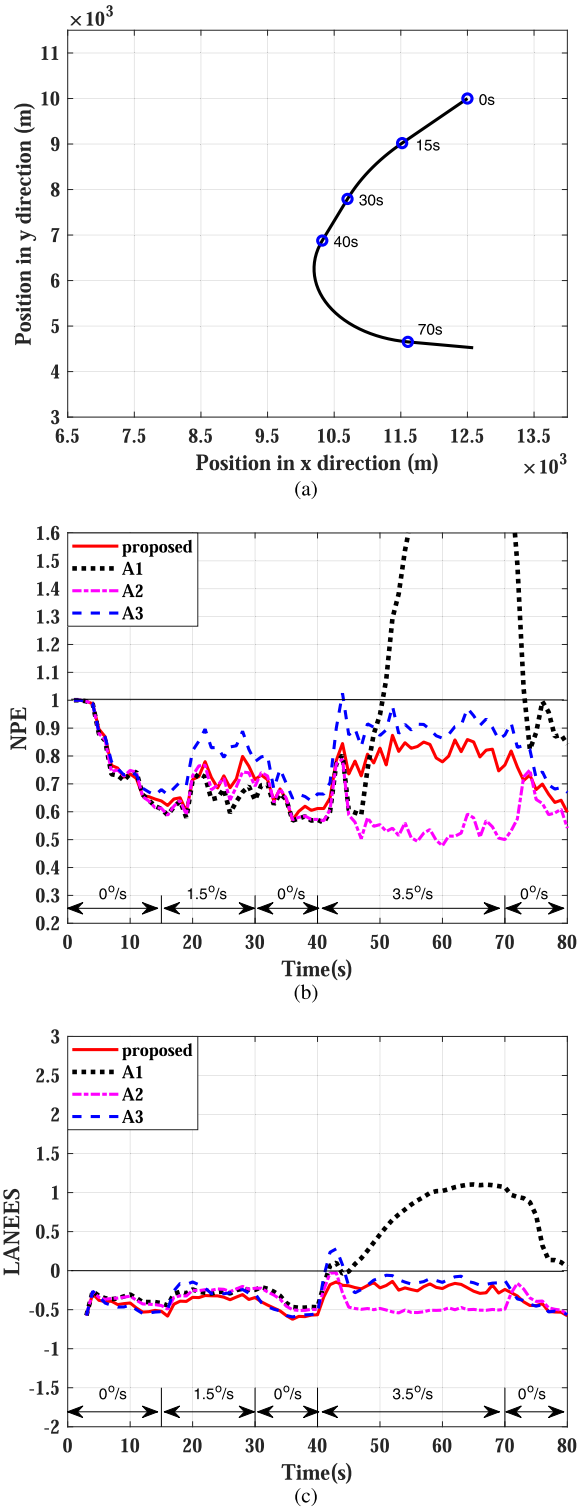

FIGURE 6. The results of the third scenario for a target that performs turns of 1.5°/s, and 3.5°/s. (a) True target trajectory. (b) Normalized position error. (c) Consistency test.

further 10 seconds. This target trajectory of this scenario is shown Fig. 4a. The initial state vector is assumed to be

$$\mathbf{x}_o = [12500\,m,\ -70.5\,m/s,\ 10000\,m,\ -70.5\,m/s]' \quad (45)$$

It is seen from Fig. 4b that all the four algorithms exhibit acceptable performance in terms of NPE. However, as expected, A1 exhibits the best performance, particularly at the second maneuver in view of the fact that the algorithm

design matches the target maneuver. In addition, it is seen from Fig. 4c that throughout the tracking period, LANEES value is always negative for all the algorithms and hence, the algorithms are consistent, except for A3, which has a positive value at the beginning of the second maneuver.

The second scenario is the same as the first one except that the second turn rate of the target is increased to $3°/s$. This scenario is depicted in Fig. 5a. From Fig. 5b, it is observed that the proposed algorithm and A2 exhibit acceptable performance throughout the tracking period. The performance of A1 deteriorates, as expected, compared to its performance in the previous scenario, since the turn rate of the target is outside the range for which the algorithm is designed. Algorithm A2 provides the best performance, as expected, since the turn rate of the target is covered in the region for which the algorithm is designed. The performance of A3 is acceptable throughout the tracking period except at the beginning of the second maneuver. As seen from Fig. 5c, the consistency of A1 is not acceptable during the second maneuver, as is to be expected. The other algorithms are consistent, but A3 again has a positive value at the beginning of the second maneuver.

In the third scenario, the second turn rate is increased to $3.5°/s$. This scenario is shown in Fig. 6a. It is seen from Figs 6b and 6c that A1 cannot track the second maneuver. As expected, A2 gives the best performance, since the turn rate of the target matches with one of the turn rates for which the algorithm has been designed. The performance of the proposed algorithm as well as that of A3 in terms of NPE and LANEES are acceptable; however, as in the previous scenarios, A3 exhibits positive value for LANEES at the beginning of the second maneuver.

In the fourth scenario, the target performs two maneuvers the first to the right at a turn rate of $-3°/s$ and the second to the left at a turn rate of $2°/s$. This scenario is shown in Fig. 7a. From Fig. 7b, it is seen that the performance of both A1 and A2 is better than that of A3 and the proposed one. As is to be expected, the performance of A1 is the best during the second maneuver, since the target turn rate is close to one of the turn rates employed in the design of the algorithm. However, the performance of A2 is the best during the first maneuver because the target turn rate is close to one of turn rates used in the design of this algorithm. Both the proposed algorithm and A3 exhibit acceptable performance in terms of NPE; however, A3 has value of more than unity for NPE at the beginning of the first maneuver. It is seen from Fig. 7c that all the algorithms have acceptable consistency, except that A1 and A3 have positive values for LANEES at the end and the beginning of the first maneuver, respectively.

The fifth scenario is the same as the fourth scenario except that the turn rate of the first maneuver is $-4.5°/s$ and that of the second is $4.5°/s$. This scenario is depicted in Fig. 8a. From Figs 8b and 8c it is seen that, as expected, both A1 and A2 are unable to track the target for either of the maneuvers, since the target turn rate is outside the ranges for which these algorithms are designed. Both the proposed algorithm and A3 show satisfactory performance in terms of the two metrics. However, A3 exhibits a positive value for LANEES at the beginning of both maneuvers, whereas the proposed algorithm has acceptable consistency throughout the tracking process.

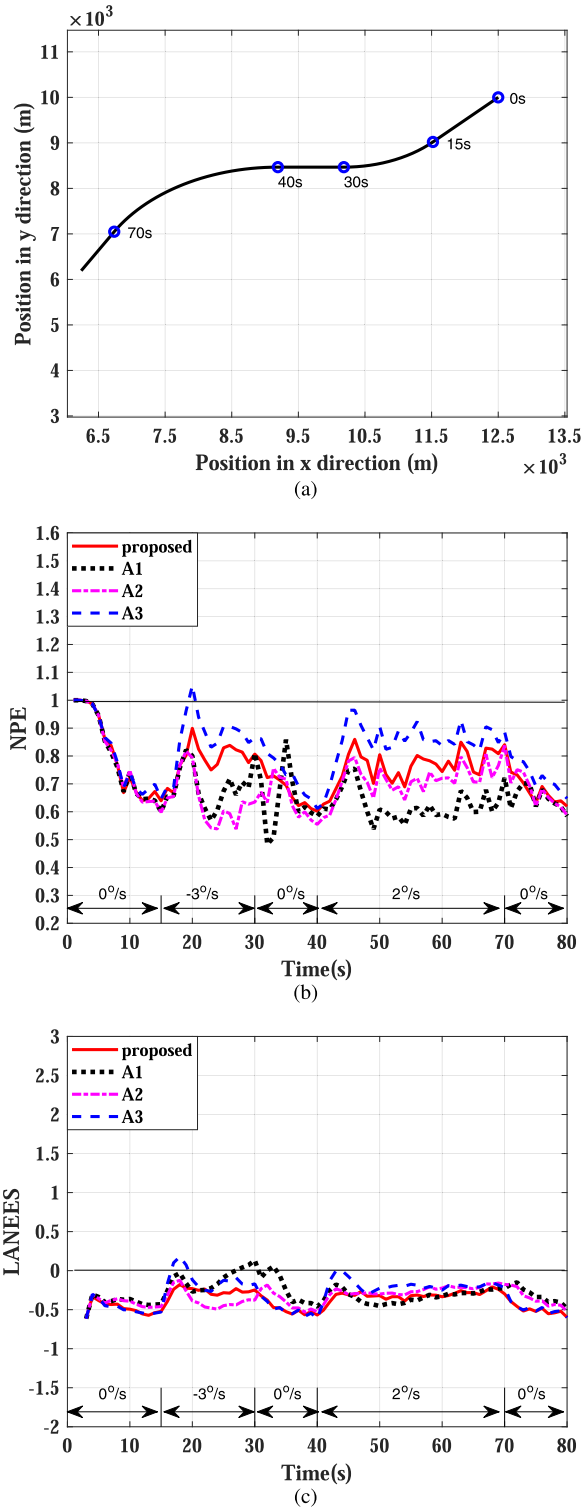

FIGURE 7. The results of the fourth scenario for a target that performs turns of $-3°/s$, and $2°/s$. (a) True target trajectory. (b) Normalized position error. (c) Consistency test.

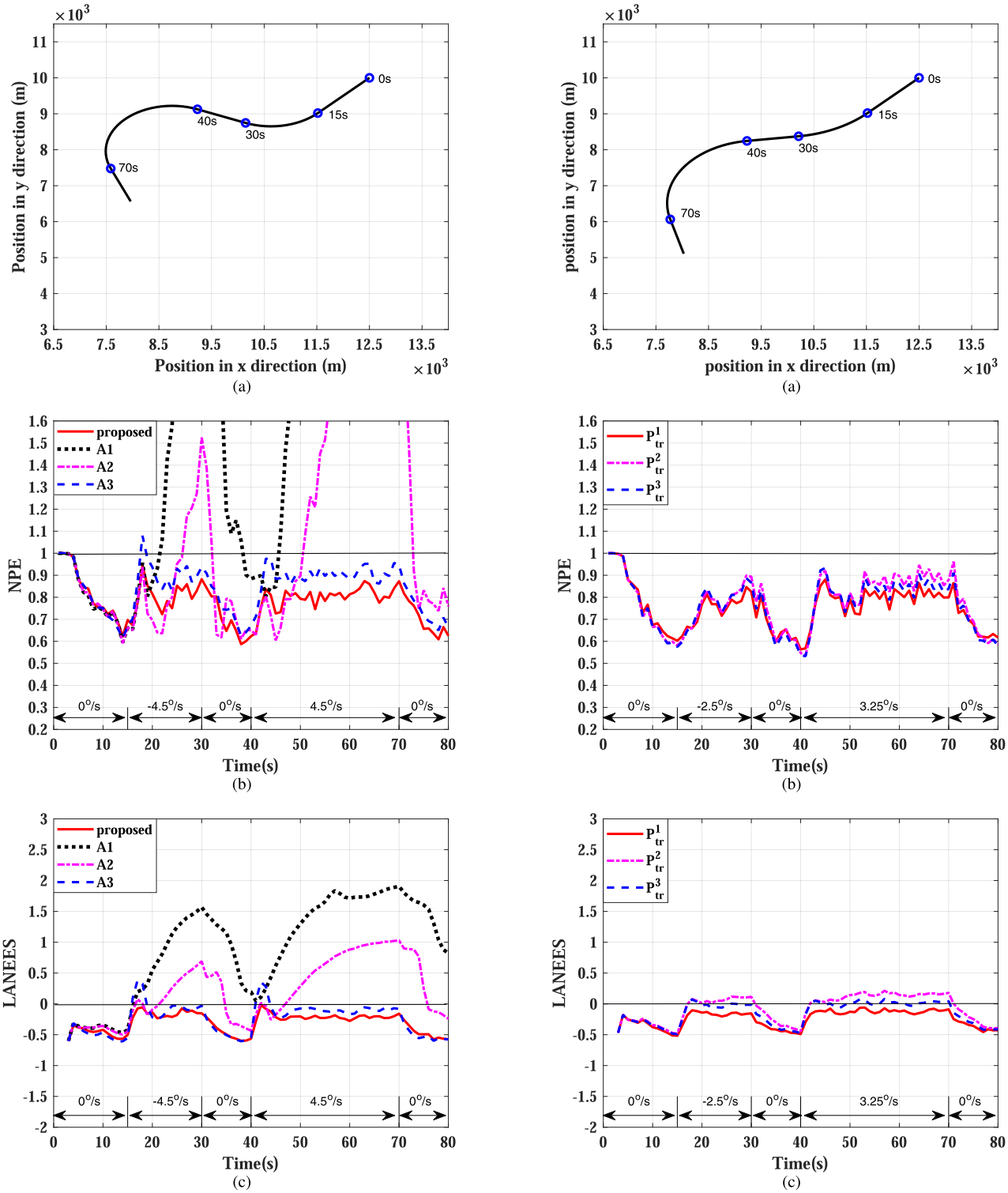

FIGURE 8. The results of the fifth scenario for a target that performs turns of $-4.5°/s$, and $4.5°/s$. (a) True target trajectory. (b) Normalized position error. (c) Consistency test.

FIGURE 9. The results of the first scenario for a target that performs turns of $-2.5°/s$, and $3.25°/s$. (a) True target trajectory. (b) Normalized position error. (c) Consistency test.

It is noticed from these scenarios that the algorithms A1 and A2 exhibit a performance better than that of A3 or the proposed algorithm, when the target turn rate is covered in the region for which these algorithms have been designed. However, when the turn rate is outside the range, then their performance may not be acceptable or they may even fail to track the target. Further, it is observed that A3 and the proposed algorithm exhibit acceptable performance in all the scenarios. But, the performance of the proposed algorithm is

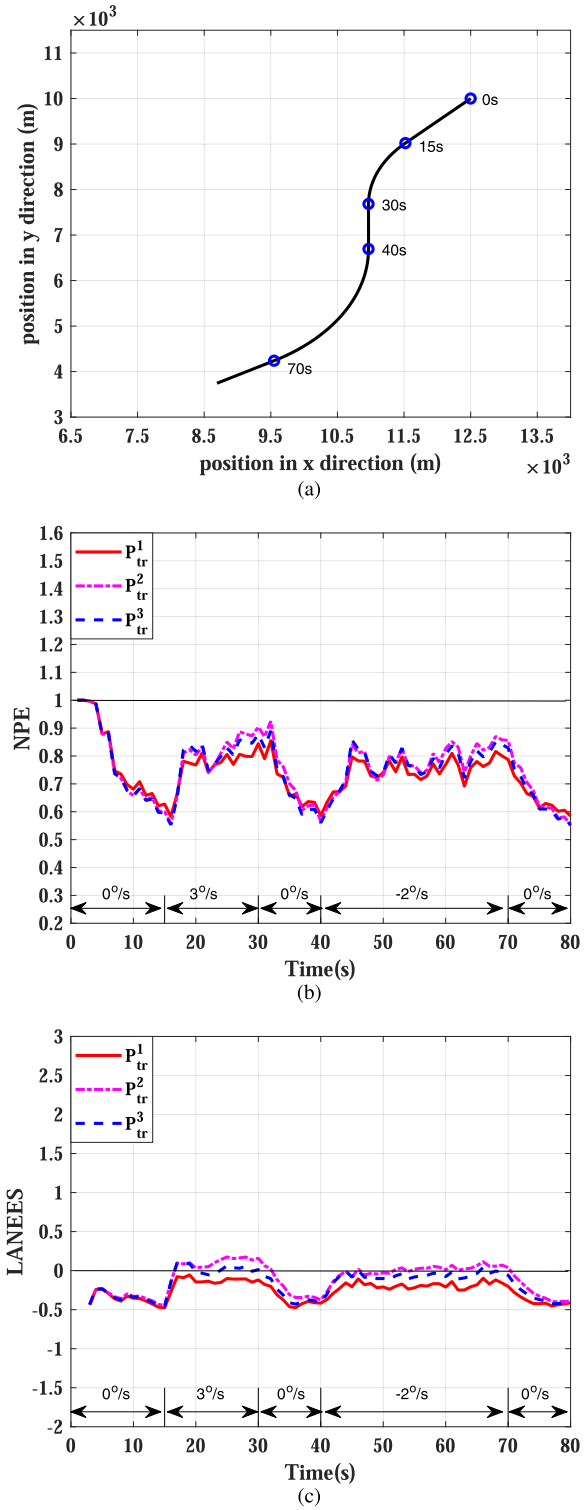

FIGURE 10. The results of the second scenario for a target that performs turns of $3°/s$, and $-2°/s$. (a) True target trajectory. (b) Normalized position error. (c) Consistency test.

always better than that of A3 during all the scenarios in terms of both NPE and the consistency, whereas the consistency of A3 may have a positive value at the beginning of a maneuver, when the turn rate is outside the range of $\pm 2°/s$. Based on these results, the proposed algorithm represents a promising performance in realistic scenarios, where prior information about the target turn rate is rarely available.

VI. CONCLUSION

In this paper, we have proposed an algorithm to track a maneuvering target, when the information on the target turn rate is not *a priori* known and the system information about only the position of the target. The turn rate is obtained adaptively based on the speed of the target and the radius of the turn using the interacting multiple model framework. We have proposed a simple method of computing the radius of the turn using the previous three consecutive measurements, assuming that the target performs a circular maneuver. A detailed study has been carried out to choose an appropriate transition probability matrix, so that the performance of the proposed algorithm is acceptable in terms of two metrics, normalized position error (NPE) and the logarithmic average normalized estimation error squared (LANEES). A comparison of the proposed algorithm with two existing algorithms has been carried out. One of these two algorithms assumes that the target turn rate is known and the other one estimates it during the tracking process. All the algorithms in this comparison use linear models, namely, the constant velocity (CV) and coordinated turn (CT) models. Based on a number of scenarios with various target turn rates, it has been shown that the proposed algorithm exhibits satisfactory performance in all of the scenarios considered, and its performance is superior to that of the adaptive algorithm. Further, when an unexpected maneuver is performed by the target, and the target turn rate is not covered by the algorithms that have been designed with a prior information on the target turn rate, the performance of these algorithms deteriorates or the algorithms may even fail to track the target, whereas the proposed algorithm always exhibits a satisfactory performance. These results foster the use of the proposed algorithm in real life situations, where the information on neither the target turn rate nor the range rate is available to the tracking algorithm.

APPENDIX A
DETERMINATION OF THE RADIUS OF THE TURN USING THREE MEASUREMENTS

In this derivation, we assume that the target performs a CT motion during the maneuvering time on the circumference of a circle with radius R_k, its center at (o_{ξ_k}, o_{η_k}) and the target moves in a straight line motion before and after the maneuver as shown in Fig. 2. Assume that three successive measurements are received. These measurements are defined as (ξ_{k-2}, η_{k-2}), (ξ_{k-1}, η_{k-1}), and (ξ_k, η_k). Therefore, these measurements will be at the same distance from the center of the turn during the maneuver motion; thus

$$R_{k-2} = R_{k-1} = R_k \tag{A.1}$$

Then, construct two equations such as

$$R_{k-2} = R_{k-1} \tag{A.2}$$

$$o_{\eta_k} = \frac{(\xi_{k-2}^2 - \xi_{k-1}^2 + \eta_{k-2}^2 - \eta_{k-1}^2)(\xi_{k-1} - \xi_k) - (\xi_{k-1}^2 - \xi_k^2 + \eta_{k-1}^2 - \eta_k^2)(\xi_{k-2} - \xi_{k-1})}{2((\eta_{k-2} - \eta_{k-1}))(\xi_{k-1} - \xi_k) - 2((\eta_{k-1} - \eta_k))(\xi_{k-2} - \xi_{k-1})} \tag{A.7}$$

$$R_{k-1} = R_k \tag{A.3}$$

From (A.3) we get

$$(\xi_k - o_{\xi_k})^2 + (\eta_k - o_{\eta_k})^2 = (\xi_{k-1} - o_{\xi_k})^2 + (\eta_{k-1} - o_{\eta_k})^2 \tag{A.4}$$

or

$$o_{\xi_k} = \frac{(\xi_{k-1}^2 - \xi_k^2) + (\eta_{k-1}^2 - \eta_k^2) - 2o_\eta(\eta_{k-1} - \eta_k)}{2(\xi_{k-1} - \xi_k)} \tag{A.5}$$

Similarly, from (A.2) we can derive that

$$o_{\xi_k} = \frac{(\xi_{k-2}^2 - \xi_{k-1}^2) + (\eta_{k-2}^2 - \eta_{k-1}^2) - 2o_\eta(\eta_{k-2} - \eta_{k-1})}{2(\xi_{k-2} - \xi_{k-1})} \tag{A.6}$$

Hence, from (A.5) and (A.6) we get (A.7), as shown at the top of this page.

Therefore, from (A.5) and (A.7), we get the center position (o_{ξ_k}, o_{η_k}). We now calculate the radius R_k using (o_{ξ_k}, o_{η_k}) and (ξ_k, η_k) as the last received information about the target.

$$R_k = \sqrt{(\xi_k - o_{\xi_k})^2 + (\eta_k - o_{\eta_k})^2} \tag{A.8}$$

APPENDIX B
DETERMINATION OF THE STATE TRANSITION MATRIX

As mentioned earlier, the target has three modes of motion, namely, straight-line motion (SL), left turning motion (LT), and right turning motion (RT), which will be referred to as modes 1, 2, and 3, respectively. The element p_{ij}, $i \neq j$ in the transition probability matrix $\mathbf{P}_{tr}$ represents the probability of the target transiting from mode i to mode j, while p_{ii} represents the probability of the target continuing to be in mode i. It has been found in [2] that p_{ii} should be between 0.8 and 0.98 for good tracking results.

We assume that p_{22} and p_{33} should have values less than p_{11} in view of the fact that we adaptively estimate ω and the predicted position by the CT models are not precise. The other elements of this matrix are adjusted such that the sum of the elements in each row is equal to unity. A number of different transition matrices and various scenarios with different maneuvers have been considered, and it has been found that the best performance in terms of both NPE and LANEES metrics is given by

$$\mathbf{P}_{tr}^1 = \begin{bmatrix} 0.9 & 0.05 & 0.05 \\ 0.1 & 0.8 & 0.1 \\ 0.1 & 0.1 & 0.8 \end{bmatrix} \tag{B.1}$$

For purpose of illustration, we consider the following two other transition matrices

$$\mathbf{P}_{tr}^2 = \begin{bmatrix} 0.95 & 0.025 & 0.025 \\ 0.2 & 0.8 & 0 \\ 0.2 & 0 & 0.8 \end{bmatrix} \tag{B.2}$$

and

$$\mathbf{P}_{tr}^3 = \begin{bmatrix} 0.95 & 0.025 & 0.025 \\ 0.15 & 0.8 & 0.05 \\ 0.15 & 0.05 & 0.8 \end{bmatrix} \tag{B.3}$$

and compare their performance with that of $\mathbf{P}_{tr}^1$ under two different scenarios.

The first scenario is shown in Fig. 9a. The target starts with a straight-line motion for 15 seconds, then performs the first maneuver to the right with a turn rate of $-2.5°/s$ for 15 seconds. Afterwards, it moves again in a straight-line motion for 10 seconds, and then performs another maneuver to the left with a turn rate of $3.25°/s$ for 30 seconds. Finally, it goes in a straight-line motion for a further 10 seconds. The initial state vector used is

$$\mathbf{x}_o = [12500\,m,\ -70.5\,m/s,\ 10000\,m,\ -70.5\,m/s]' \tag{B.4}$$

The algorithm with $\mathbf{P}_{tr}^1$ shows a better tracking performance during the maneuvers in terms of NPE, as shown in Fig. 9b, compared to that of the algorithm with $\mathbf{P}_{tr}^2$ or $\mathbf{P}_{tr}^3$. It is clear from Fig. 9c the algorithm with $\mathbf{P}_{tr}^1$ preserves its consistency throughout the tracking period, while the other two do not in the sense that LANEES for these two becomes positive during the maneuvers.

The second scenario is the same as the first one except for the maneuvering turn rates; the first maneuver is performed to the left with a turn rate of $3°/s$ and the second maneuver to the right with a turn rate of $-2°/s$, as shown in Fig. 10a. It is see from Fig. 10b and Fig. 10c that the conclusions made regarding NPE and consistency of the algorithm with $\mathbf{P}_{tr}^1$, $\mathbf{P}_{tr}^2$ and $\mathbf{P}_{tr}^3$ for the previous scenario hold good for the present scenario also.

From the above two scenarios, it is clear that the performance of the algorithm in terms of both NPE and LANEES is better with $\mathbf{P}_{tr}^1$ as the transition probability matrix than with $\mathbf{P}_{tr}^2$ or $\mathbf{P}_{tr}^3$. Similar performance of $\mathbf{P}_{tr}^1$ has been observed in other scenarios and with other transition probability matrices, but are not reported here. In view of these findings, we choose $\mathbf{P}_{tr}^1$ as the proposed transition probability matrix and denote it by $\mathbf{P}_{tr}^{prop}$.

REFERENCES

[1] X. R. Li and V. P. Jilkov, "Survey of maneuvering target tracking: Decision-based methods," *Proc. SPIE*, vol. 4728, Aug. 2002, pp. 511–534.

[2] Y. Bar-Shalom, X. R. Li, and T. Kirubarajan, *Estimation With Applications to Tracking and Navigation: Theory Algorithms and Software*. New York, NY, USA: Wiley, 2004.

[3] Y. Bar-Shalom and K. Birmiwal, "Variable dimension filter for maneuvering target tracking," *IEEE Trans. Aerosp. Electron. Syst.*, vols. AES–18, no. 5, pp. 621–629, Sep. 1982.
[4] T. Kirubarajan and Y. Bar-Shalom, "Kalman filter versus IMM estimator: When do we need the latter?" *IEEE Trans. Aerosp. Electron. Syst.*, vol. 39, no. 4, pp. 1452–1457, Oct. 2003.
[5] X. R. Li and Y. Bar-Shalom, "Design of an interacting multiple model algorithm for air traffic control tracking," *IEEE Trans. Control Syst. Technol.*, vol. 1, no. 3, pp. 186–194, Sep. 1993.
[6] M. Silbert, S. Sarkani, and T. Mazzuchi, "Comparing the state estimates of a Kalman filter to a perfect IMM against a maneuvering target," in *Proc. 14th Int. Conf. Inf. Fusion*, Jul. 2011, pp. 1–5.
[7] G. Ackerson and K. Fu, "On state estimation in switching environments," *IEEE Trans. Autom. Control*, vol. AC-15, no. 1, pp. 10–17, Feb. 1970.
[8] C. Chang and M. Athans, "State estimation for discrete systems with switching parameters," *IEEE Trans. Aerosp. Electron. Syst.*, vol. AES-14, no. 3, pp. 418–425, May 1978.
[9] J. K. Tugnait, "Comments on," state estimation for discrete systems with switching parameters," *IEEE Trans. Aerosp. Electron. Syst.*, vol. AES-15, no. 3, p. 464, May 1979.
[10] H. A. P. Blom and Y. Bar-Shalom, "The interacting multiple model algorithm for systems with markovian switching coefficients," *IEEE Trans. Autom. Control*, vol. AC-33, no. 8, pp. 780–783, Aug. 1988.
[11] G. Xie, L. Sun, T. Wen, X. Hei, and F. Qian, "Adaptive transition probability matrix-based parallel IMM algorithm," *IEEE Trans. Syst., Man, Cybern. Syst.*, early access, Jun. 27, 2019, doi: 10.1109/TSMC.2019.2922305.
[12] K. Watanabe and S. G. Tzafestas, "Generalized pseudo-bayes estimation and detection for abruptly changing systems," *J. Intell. Robotic Syst.*, vol. 7, no. 1, pp. 95–112, Feb. 1993.
[13] X.-R. Li and Y. Bar-Shalom, "Multiple-model estimation with variable structure," *IEEE Trans. Autom. Control*, vol. 41, no. 4, pp. 478–493, Apr. 1996.
[14] A. F. Genovese, "The interacting multiple model algorithm for accurate state estimation of maneuvering targets," *Johns Hopkins APL Tech. Dig.*, vol. 22, no. 4, pp. 614–623, 2001.
[15] A. Munir, J. A. Mirza, and A. Q. Khan, "Parameter adjustment in the turn rate models in the interacting multiple model algorithm to track a maneuvering target," in *Proc. IEEE Int. Multi Topic Conf. INMIC Technol. 21st Century*, Dec. 2001, pp. 262–266.
[16] Y. He, J. Xiu, and X. Guan, *Radar Data Processing With Applications*. Singapore: Wiley, 2016.
[17] Y. Bar-Shalom, *Multitarget-Multisensor Tracking: Advanced Applications*. Norwood, MA, USA, Artech House, 1990, p. 391.
[18] A. Munir and D. P. Atherton, "Maneuvring target tracking using different turn rate models in the interacting multiple model algorithm," in *Proc. 34th IEEE Conf. Decis. Control*, Dec. 1995, pp. 2747–2751.
[19] R. Visina, Y. Bar-Shalom, and P. Willett, "Multiple-model estimators for tracking sharply maneuvering ground targets," *IEEE Trans. Aerosp. Electron. Syst.*, vol. 54, no. 3, pp. 1404–1414, Jun. 2018.
[20] X. Yuan, C. Han, Z. Duan, and M. Lei, "Adaptive turn rate estimation using range rate measurements," *IEEE Trans. Aerosp. Electron. Syst.*, vol. 42, no. 4, pp. 1532–1541, Oct. 2006.
[21] L. Zhu and X. Cheng, "High manoeuvre target tracking in coordinated turns," *IET Radar, Sonar Navigat.*, vol. 9, no. 8, pp. 1078–1087, Oct. 2015.
[22] V. B. Frencl, J. B. R. do Val, R. S. Mendes, and Y. C. Zuñiga, "Turn rate estimation using range rate measurements for fast manoeuvring tracking," *IET Radar, Sonar Navigat.*, vol. 11, no. 7, pp. 1099–1107, Jul. 2017.
[23] F. A. Administration and U. S. F. A. Administration, *Pilot's Handbook of Aeronautical Knowledge*. New York, NY, USA: Skyhorse, 2016.
[24] B. Han, H. Huang, L. Lei, C. Huang, and Z. Zhang, "An improved IMM algorithm based on STSRCKF for maneuvering target tracking," *IEEE Access*, vol. 7, pp. 57795–57804, 2019.
[25] M. Zarei-Jalalabadi and S. M.-B. Malaek, "Modification of unscented Kalman filter using a set of scaling parameters," *IET Signal Process.*, vol. 12, no. 4, pp. 471–480, Jun. 2018.
[26] X. Rong Li and V. P. Jilkov, "Survey of maneuvering target tracking. Part I. Dynamic models," *IEEE Trans. Aerosp. Electron. Syst.*, vol. 39, no. 4, pp. 1333–1364, Oct. 2003.
[27] A. Farina and S. Pardini, "Survey of radar data-processing techniques in air-traffic-control and surveillance systems," *IEE Proc. F Commun., Radar Signal Process.*, vol. 127, no. 3, pp. 190–204, Jun. 1980.
[28] S. V. Bordonaro, P. Willett, and Y. Bar-Shalom, "Unbiased tracking with converted measurements," in *Proc. IEEE Radar Conf.*, May 2012, pp. 0741–0745.
[29] R. A. Best and J. P. Norton, "A new model and efficient tracker for a target with curvilinear motion," *IEEE Trans. Aerosp. Electron. Syst.*, vol. 33, no. 3, pp. 1030–1037, Jul. 1997.
[30] M. B. Rhudy, R. A. Salguero, and K. Holappa, "A Kalman filtering tutorial for undergraduate students," *Int. J. Comput. Sci. Eng. Surv.*, vol. 8, no. 1, pp. 1–18, 2017.
[31] E. Mazor, A. Averbuch, Y. Bar-Shalom, and J. Dayan, "Interacting multiple model methods in target tracking: A survey," *IEEE Trans. Aerosp. Electron. Syst.*, vol. 34, no. 1, pp. 103–123, Jan. 1998.
[32] D. S. Pietro. *Relating Angular and Regular Motion Variables*. Accessed: Nov. 2019. [Online]. Available: https://www.khanacademy.org/science/physics/torque-angular-momentum/rotational-kinematics/v/relating-angular-and-regular-motion-variables
[33] A. Ruina and R. Pratap. (Oct. 2019). *Introduction to Statics and Dynamics*. [Online]. Available: http://ruina.tam.cornell.edu/Book

MOHAMED ELTOUKHY received the B.Sc. and M.Sc. degrees in electrical engineering from the Military Technical College (MTC), Cairo, Egypt, in 2005 and 2013, respectively. He is currently pursuing the Ph.D. degree with the Electrical and Computer Engineering Department, Concordia University, Montreal, QC, Canada. From 2005 to 2017, he was a Research Assistant with the Technical Research Center (TRC), Cairo. His research interests include adaptive filters, data association, and data processing. His current research interest includes tracking multiple targets in a cluttered environment. He has been a member of the Laboratory of Signal Processing, Concordia University, since 2018. He received a number of awards such as the Egyptian MoD Scholarship in the periods, from 2010 to 2013 and from 2018 to 2021.

M. OMAIR AHMAD (Life Fellow, IEEE) received the B.Eng. degree in electrical engineering from Sir George Williams University, Montreal, QC, Canada, and the Ph.D. degree in electrical engineering from Concordia University, Montreal. From 1978 to 1979, he was a Faculty Member with the New York University College, Buffalo, NY, USA. In 1979, he joined the Faculty of Concordia University, as an Assistant Professor of computer science. Subsequently, he joined the Department of Electrical and Computer Engineering, Concordia University, where he was the Chair, from 2002 to 2005, where he is currently a Professor. He was a Guest Professor with Southeast University, Nanjing, China. He was a Founding Researcher of Micronet and a Canadian Network of Centers of Excellence, from 1990 to 2004. He is also the Concordia University Research Chair (Tier I) of multimedia signal processing. He has authored in the area of signal processing. He holds four patents. His current research interests include the areas of image and speech processing, biomedical signal processing, watermarking, biometrics, video signal processing and object detection and tracking, deep learning techniques in signal processing, and fast signal transforms and algorithms. In 1988, he was a member of the Admission and Advancement Committee of the IEEE. He was a recipient of numerous honors and awards, including the Wighton Fellowship from the Sandford Fleming Foundation, an induction to Provosts Circle of Distinction for Career Achievements, and the Award of Excellence in Doctoral Supervision from the Faculty of Engineering and Computer Science, Concordia University. He was the Local Arrangements Chairman of the 1984 IEEE International Symposium on Circuits and Systems. He has served as the Program Co-Chair for the 1995 IEEE International Conference on Neural Networks and Signal Processing, the 2003 IEEE International Conference on Neural Networks and Signal Processing, and the 2004 IEEE International Midwest Symposium on Circuits and Systems. He was the General Co-Chair of the 2008 IEEE International Conference on Neural Networks and Signal Processing. He is the Chair of the Montreal Chapter IEEE Circuits and Systems Society. He was an Associate Editor of the IEEE TRANSACTIONS ON CIRCUITS AND SYSTEMS—I: FUNDAMENTAL THEORY AND APPLICATIONS, from 1999 to 2001.

M. N. S. SWAMY (Life Fellow, IEEE) received the B.Sc. degree (Hons.) in mathematics from the University of Mysore, Mysore, India, in 1954, the Diploma degree in electrical communication engineering from the Indian Institute of Science, Bengaluru, India, in 1957, and the M.Sc. and Ph.D. degrees in electrical engineering from the University of Saskatchewan, Saskatoon, SK, Canada, in 1960 and 1963, respectively. He was conferred with the title of Honorary Professor by the National Chiao Tung University, Hsinchu, Taiwan, in 2009. He is currently a Research Professor with the Department of Electrical and Computer Engineering, Concordia University, Montreal, QC, Canada, where he served as the Founding Chair of the Department of Electrical Engineering, from 1970 to 1977, and the Dean of engineering and computer science, from 1977 to 1993. During that time, he has developed the faculty into a research oriented one, from what was primarily as an undergraduate faculty. Since 2001, he has been the Concordia Chair (Tier I) of signal processing. He has also taught at the Department of Electrical Engineering, Technical University of Nova Scotia, Halifax, NS, Canada, the University of Calgary, Calgary, AB, Canada, and the Department of Mathematics, University of Saskatchewan. He has published in the areas of number theory, circuits, systems, and signal processing. He holds five patents. He has coauthored nine books and five book chapters. He served as a member for the Board of Governors of the CAS Society. He was a Founding Member of Micronet, a Canadian Network of Centers of Excellence, from 1990 to 2004, and also its Coordinator of Concordia University. He is a Fellow of the Institute of Electrical Engineers, U.K., the Engineering Institute of Canada, the Institution of Engineers, India, and the Institution of Electronic and Telecommunication Engineers, India. He was inducted to the Provosts Circle of Distinction for career achievements, in 2009. He was a recipient of many IEEE-CAS Society Awards, including the 1986 Guillemin-Cauer Best Paper Award Education Award, in 2000, and the Golden Jubilee Medal, in 2000. He has served as the Program Chair for the 1973 IEEE Circuits and Systems (CAS) Symposium, the General Chair for the 1984 IEEE CAS Symposium, and the Vice Chair for the 1999 IEEE CAS Symposium. He has been the Editor-in-Chief of the Circuits, Systems, and Signal Processing (CSSP) journal, since 1999. Recently, the CSSP has instituted the Best Paper Award in his name. He has served as the Editor-in-Chief for the IEEE TRANSACTIONS ON CIRCUITS AND SYSTEMS—I, from 1999 to 2001, and an Associate Editor for the IEEE TRANSACTIONS ON CIRCUITS AND SYSTEMS, from 1985 to 1987. He has served the IEEE in various capacities, such as the President Elect, in 2003, the President, in 2004, the Past-President, in 2005, the Vice President (publications), from 2001 to 2002, and the Vice President, in 1976.